

## Supporting Information

### **Hyaluronic Acid Nanoparticles Based on Conjugated Oligmer Photosensitizer: Target-specific Two-photon Imaging, Redox-sensitive Drug Delivery and Synergistic Chemo-photodynamic Therapy**

Yan-Qin Huang,<sup>1,\*</sup> Li-Jie Sun,<sup>1</sup> Rui Zhang,<sup>4,\*</sup> Jian Hu,<sup>1</sup> Xing-Fen Liu,<sup>1</sup> Rong-Cui Jiang,<sup>1</sup>  
Qu-Li Fan,<sup>1</sup> Lian-Hui Wang,<sup>1</sup> Wei Huang<sup>1,2,3\*</sup>

(1. Key Laboratory for Organic Electronics & Information Displays (KLOEID) and  
Institute of Advanced Materials (IAM), Jiangsu National Synergetic Innovation Center  
for Advanced Materials (SICAM), Nanjing University of Posts & Telecommunications,  
Nanjing 210023, China.

2. Shaanxi Institute of Flexible Electronics (SIFE), Northwestern Polytechnical  
University (NPU), 127 West Youyi Road, Xi'an 710072, China

3. Key Laboratory of Flexible Electronics (KLOFE) & Institute of Advanced Materials  
(IAM), Jiangsu National Synergetic Innovation Center for Advanced Materials  
(SICAM), Nanjing Tech University (NanjingTech), Nanjing 211816, China

4. Department of Ophthalmology, Zhongda Hospital, Southeast University, Nanjing  
210009, China.)

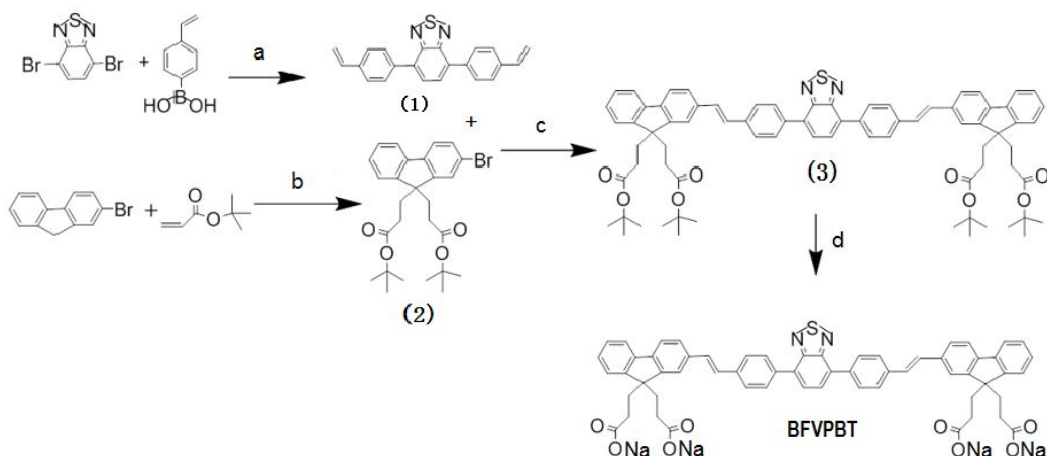
---

\* To whom correspondence should be addressed: E-mail: iamyqhuang@njupt.edu.cn,  
Tel/Fax: +86 25 8586 6396/8586 6396; E-mail: provost@nwpu.edu.cn, Tel/Fax: +86  
25 8586 6396/8586 6396.

## Table of Contents

1. Synthesis and characterization of BFVPBT .....	S-3
(1) <i>Synthesis and characterization of Compound 1 (1)</i> .....	S-4
(2) <i>Synthesis and characterization of Compound 2 (2)</i> .....	S-4
(3) <i>Synthesis and characterization of Compound 3 (3)</i> .....	S-5
(4) <i>Synthesis and characterization of BFVPBT</i> .....	S-6
2. Photograph of the product HA-SS-BFVPBT after freeze-drying.....	S-6
3. Standard curve obtained from the CPT UV-Vis absorption spectra .....	S-7
4. Standard curve obtained from the BFVPBT UV-Vis absorption spectra .....	S-7
5. FT-IR spectra of HA, HA-Cystamine, BFVPBT and HA-SS-BFVPBT .....	S-8
6. Critical micelle concentration (CMC) determination of HA-SS-BFVPBT by pyrene fluorescence spectroscopy .....	S-8
7. TEM image of CPT-loaded HSBNPs .....	S-9
8. Photograph of the aqueous solutions of HA-SS-BFVPBT, free CPT and CPT- loaded HSBNPs .....	S-9
9. Stability of CPT-loaded HSBNPs under physiological conditions .....	S-9
10. Photostability of HSBNPs in two-photon fluorescence cell imaging .....	S-10
11. Control experiments for the detection of singlet oxygen .....	S-11
12. Cytotoxicity of HSBNPs against HeLa cells .....	S-12

## 1. Synthesis and characterization of BFVPBT



Scheme S1. Synthetic routes for BFVPBT. Reagents and conditions: (a) 4-vinylphenylboronic acid,  $\text{Pd}(\text{pph}_3)_4$ , 1,4-dioxane,  $\text{K}_2\text{CO}_3$ , 100 °C, 24 h; (b) TBAB, KOH, tert-butyl acrylate, toluene, 5 h, rt; (c)  $\text{Pd}(\text{OAc})_2$ ,  $\text{P}(o\text{-tolyl})_3$ , DMF, triethylamine rt, 110 °C, 24 h; (d) trifluoroacetic acid,  $\text{CH}_2\text{Cl}_2$ , rt, overnight,  $\text{Na}_2\text{CO}_3$ , 4 h.

BFVPBT was designed to exhibit donor-bridge-acceptor-bridge-donor (D- $\pi$ -A- $\pi$ -D) architecture. As shown in Scheme S1, fluorene served as the donor, benzothiazole was the acceptor, and phenylvinylene was selected as the bridge due to its good molecular coplanarity, which had been proven favorable to two-photon absorption and redshifted emission.<sup>1-5</sup> In the synthetic route for BFVPBT, the divinyl Compound 1 was synthesized in 72% yield via the Suzuki coupling reaction between 4,7-dibromo-2,1,3-benzothiadiazole and 4-vinylphenylboronic acid in 1,4-dioxane. Compound 2 was synthesized according to the previous reports.<sup>6</sup> Direct alkylation of 2,7-dibromofluorene using tert-butyl acrylate in a mixture of toluene/aqueous KOH gave compound 2 in 52% yield. A  $\text{Pd}(\text{OAc})_2/\text{P}(o\text{-tolyl})_3$  catalyzed Heck coupling reaction of Compound 1 with Compound 2 in the mixture of DMF/TEA (1:1) at 110 °C afforded the neutral compound 3.<sup>7</sup> Then, hydrolysis of the ester groups of Compound 3 occurred in a mixture of  $\text{CH}_2\text{Cl}_2$  and trifluoroacetic acid at room temperature. After solvent evaporation, the residue was treated with aqueous  $\text{Na}_2\text{CO}_3$ , and the anionic BFVPBT was thus obtained in a yield of 81%.<sup>6</sup> Detailed steps are as follows.

### (1) Synthesis and characterization of Compound 1 (1)

4,7-Dibromo-2,1,3-benzothiadiazole (0.82 g, 2.8 mmol), 4-vinylphenylboronic acid (1 g, 6.7 mmol) and Pd(pph<sub>3</sub>)<sub>4</sub> (161 mg, 0.14 mmol) were mixed together and protected by nitrogen in a round-bottom flask in the dark. The flask was degassed with three vacuum-nitrogen cycles to remove air. Then, 1,4-dioxane (12 mL) and K<sub>2</sub>CO<sub>3</sub> (2 M, 6 mL) were added using injectors. The reaction mixture was stirred for 24 h at 100 °C under a nitrogen atmosphere, and then cooled to room temperature. After being extracted with CH<sub>2</sub>Cl<sub>2</sub>, the separated organic layer was washed with water and dried over Mg<sub>2</sub>SO<sub>4</sub>. After the solvent was evaporated, the crude product was purified by silica-gel column chromatography using petroleum ether and ethyl acetate (80:1) as the eluent to give **1** as light yellow powder (0.68g, yield: 72%). <sup>1</sup>H NMR (400 MHz, CDCl<sub>3</sub>): δ 7.96 (d, J = 8.3 Hz, 4H), 7.79 (s, 2H), 7.60 (d, J = 8.2 Hz, 4H), 6.82 (dd, J = 17.6, 10.9 Hz, 2H), 5.86 (d, J = 17.6 Hz, 2H), 5.34 (d, J = 10.9 Hz, 2H). HRMS (EI): Calcd for C<sub>22</sub>H<sub>16</sub>N<sub>2</sub>S, 340.4408; Found, 340.4416. Anal. Calcd for C<sub>22</sub>H<sub>16</sub>N<sub>2</sub>S: C, 77.62; H, 4.74; N, 8.23. Found: C, 77.51; H, 4.66; N, 8.11.

*(2) Synthesis and characterization of Compound 2 (2)*

KOH aqueous solution (2.5 mL, 50 wt%) was added dropwise to a mixed solution of 2-bromofluorene (1.11 mg, 4.5 mmol) and tetrabutylammonium bromide (TBAB, 187 mg, 0.58 mmol) in toluene (8 mL) at room temperature. After stirring for 20 min, tert-butyl acrylate (2.44 g, 18.9 mmol) was added dropwise to the mixed solution, and the mixture was stirred for 5 h at room temperature. After being extracted with CH<sub>2</sub>Cl<sub>2</sub>, the separated organic layer was washed with water and dried over Mg<sub>2</sub>SO<sub>4</sub>. After the solvent was evaporated, the crude product was purified by silica-gel column chromatography using petroleum ether and ethyl acetate (80:1) as the eluent to give **2** as transparent oil, which became solid after being placed for a period of time (1.16 g, yield: 52%). <sup>1</sup>H NMR (400 MHz, CDCl<sub>3</sub>): δ 7.69 – 7.64 (m, 1H), 7.56 (d, J = 8.0 Hz, 1H), 7.51 – 7.46 (m, 2H), 7.39 – 7.32 (m, 3H), 2.39 – 2.25 (m, 4H), 1.50 – 1.42 (m, 4H), 1.31 (s, 18H). HRMS (EI): Calcd for C<sub>27</sub>H<sub>33</sub>BrO<sub>4</sub>, 501.4525; Found, 501.4517. Anal. Calcd for C<sub>27</sub>H<sub>33</sub>BrO<sub>4</sub>: C, 64.60; H, 6.58. Found: C, 64.37; H, 6.41.

*(3) Synthesis and characterization of Compound 3 (3)*

In the dark, a Schlenk tube was charged with **1** (0.34 mg, 1mmol), **2** (1.103 mg, 2.2

mmol), P(o-tolyl)<sub>3</sub> (30mg, 0.1 mmol), and Pd(OAc)<sub>2</sub> (11mg, 0.05 mmol) under nitrogen, and then it was sealed with a rubber septum. The Schlenk tube was degassed with three vacuum-nitrogen cycles to remove air. Then, DMF (5 mL) and triethylamine (5 mL) were added to the Schlenk tube. The reaction mixture was stirred for 24 h at 110 °C under a nitrogen atmosphere. After being extracted with CH<sub>2</sub>Cl<sub>2</sub>, the separated organic layer was washed with water and dried over Mg<sub>2</sub>SO<sub>4</sub>. After the solvent was evaporated, the crude product was purified by silica-gel column chromatography using petroleum ether and ethyl acetate (40:1) as the eluent to give 3 as orange crystalline powder (0.66g, yield: 56%). <sup>1</sup>H NMR (400 MHz, CDCl<sub>3</sub>): δ 8.08 (d, J = 8.4 Hz, 4H), 7.89 (s, 2H), 7.75 (dd, J = 17.4, 7.9 Hz, 8H), 7.59 (d, J = 8.0 Hz, 4H), 7.39 (m, 6H), 7.32 (s, 4H), 2.50 – 2.34 (m, 8H), 1.55 (m, 8H), 1.33 (s, 36H). HRMS (MALDI-TOF): Calcd for C<sub>76</sub>H<sub>80</sub>N<sub>2</sub>O<sub>8</sub>S, 1181.5220; Found, 1181.5225. Anal. Calcd for C<sub>76</sub>H<sub>80</sub>N<sub>2</sub>O<sub>8</sub>S: C, 77.26; H, 6.82; N, 2.37. Found: C, 77.37; H, 6.79; N, 2.25.

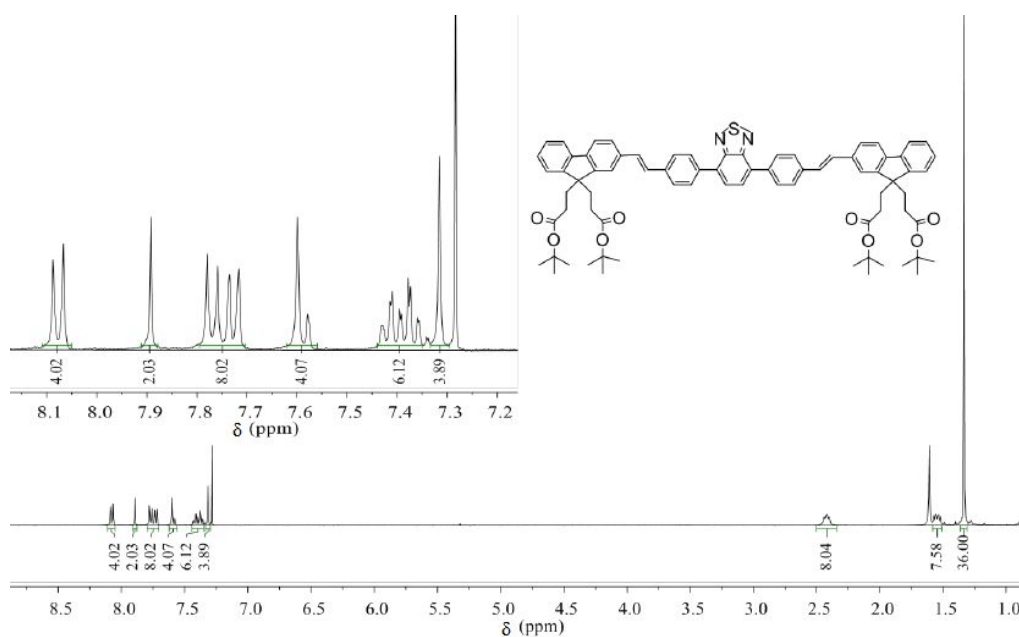


Figure S1. <sup>1</sup>H NMR spectrum of Compound 3.

#### (4) Synthesis and characterization of BFVPBT

Compound 3 (0.38 g, 0.32 mmol), trifluoroacetic acid (20 ml) and CH<sub>2</sub>Cl<sub>2</sub> (100ml) were mixed in a round-bottom flask. The reaction mixture was stirred at room temperature overnight. After the solvent was evaporated, Na<sub>2</sub>CO<sub>3</sub> (20ml, 0.05M) was added to the flask and stirred for 4 h. The mixture was filtered and washed with

petroleum ether to give BFVPBT as orange solid (0.25g, yield: 81%).  $^1\text{H}$  NMR (400 MHz, DMSO- $d_6$ )  $\delta$  8.11 (d,  $J$  = 8.4 Hz, 4H), 8.04 (s, 2H), 7.84 (m, 10H), 7.66 (d,  $J$  = 8.3 Hz, 2H), 7.56 – 7.43 (m, 6H), 7.42 – 7.31 (m, 4H), 2.36 (m, 8H), 1.37 (m, 8H).  $^{13}\text{C}$  NMR (100 MHz, DMSO- $d_6$ ):  $\delta$  (ppm) 174.4, 153.9, 149.1, 148.8, 140.8, 137.7, 137.0, 136.3, 132.2, 129.9, 128.6, 128.1, 127.1, 123.6, 121.2, 120.9, 120.7. Anal. Calcd for  $\text{C}_{60}\text{H}_{44}\text{N}_2\text{Na}_4\text{O}_8\text{S}$ : C, 68.96; H, 4.24; N, 2.68. Found: C, 68.77; H, 4.12; N, 2.55.

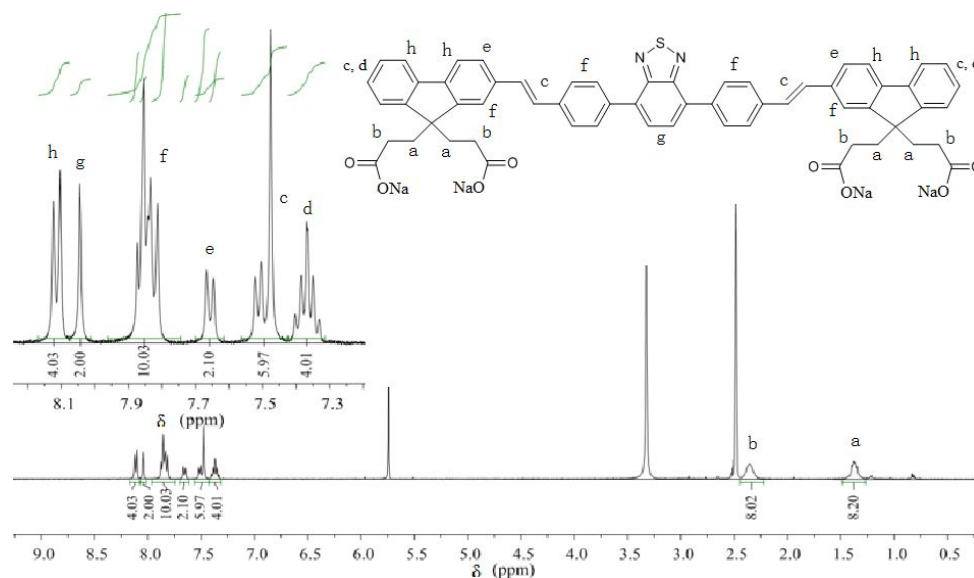


Figure S2.  $^1\text{H}$  NMR spectrum of BFVPBT.

With each fluorene ring containing two carboxylate groups, BFVPBT could be readily dissolved in polar solvents, such as DMF, DMSO, and methanol. In the  $^1\text{H}$  NMR spectrum of BFVPBT (Figure S2), there was no residual peak observed at  $\sim 1.33$  ppm that corresponded to  $-\text{COOC}(\text{CH}_3)_3$  in compound 3 (Figure S2), which indicated that nearly all of  $-\text{COOC}(\text{CH}_3)_3$  was converted to  $-\text{COONa}$ .<sup>8,9</sup>

## 2. Photograph of the product HA-SS-BFVPBT after freeze-drying



Figure S3. Product of HA-SS-BFVPBT after freeze-drying.

### 3. Standard curve obtained from the CPT UV-vis absorption spectra

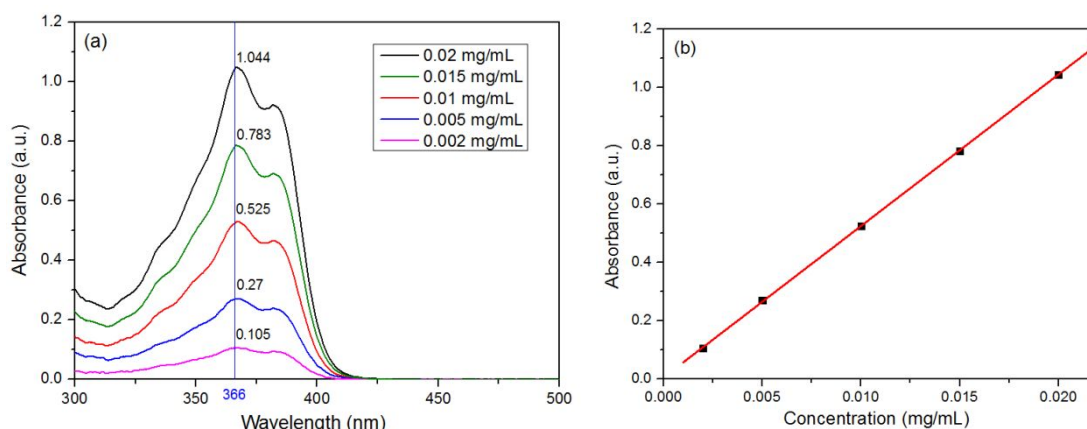


Figure S4. (a) UV-Vis absorption spectra of DMF solutions of CPT with different concentrations. (b) Standard curve at 366 nm obtained from the UV-Vis absorbance of the above solutions.

### 4. Standard curve obtained from the BFVPBT UV-Vis absorption spectra

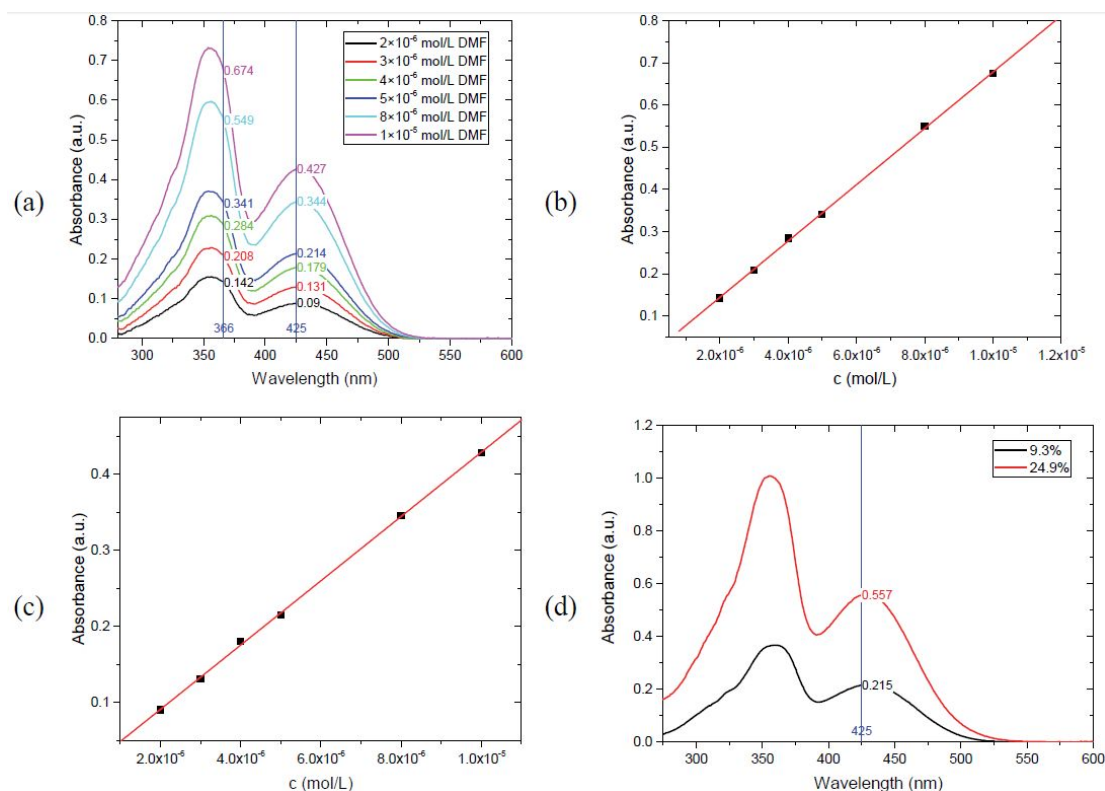


Figure S5. (a) UV-Vis absorption spectra of DMF solutions of BFVPBT with different concentrations. (b) Standard curve at 366 nm obtained from the UV-Vis absorbance of the above solutions. (c) Standard curve at 425 nm obtained from the UV-Vis absorbance of the above solutions. (d) UV-Vis absorption spectra of HA-SS-BFVPBT with different degree of substitutions (DS) calculated according to the standard curve at 425

nm.

## 5. FT-IR spectra of HA, HA-Cystamine, BFVPBT and HA-SS-BFVPBT

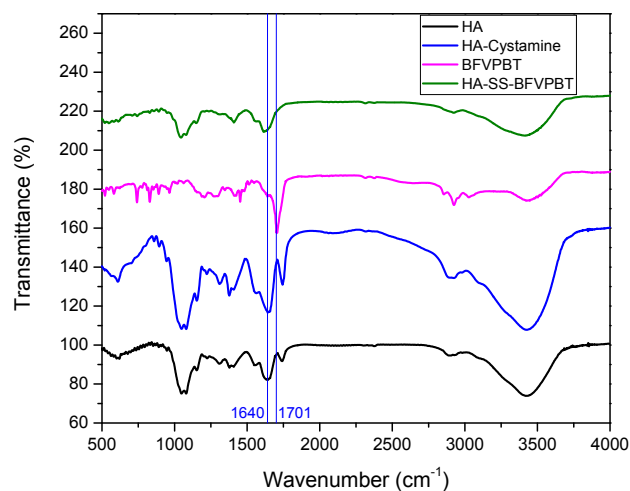


Figure S6. FT-IR spectra of HA, HA-Cystamine, BFVPBT and HA-SS-BFVPBT.

## 6. Critical micelle concentration (CMC) determination of HA-SS-BFVPBT by pyrene fluorescence spectroscopy

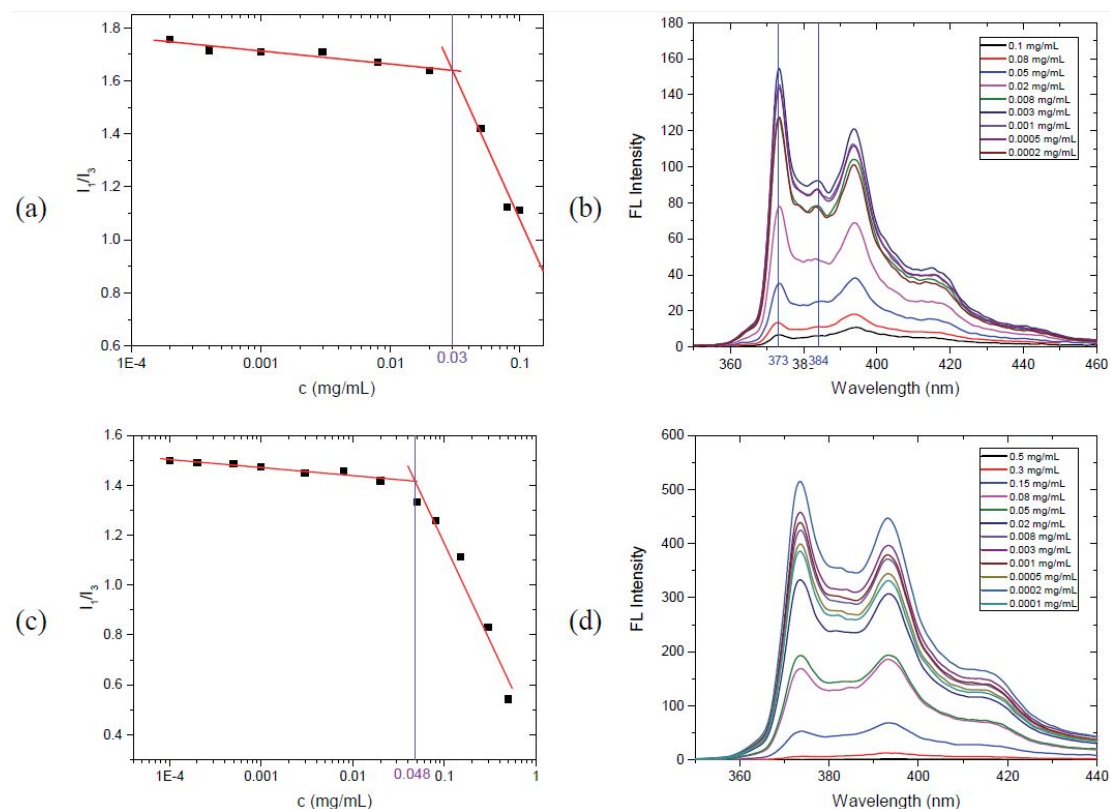


Figure S7. Critical micelle concentration (CMC) determination of (a) HA-SS-BFVPBT with 24.9% DS or (c) HA-SS-BFVPBT with 9.3% DS. Fluorescence spectra of pyrene with the addition of (b) HA-SS-BFVPBT (DS = 24.9%) or (d) HA-SS-BFVPBT (DS =



9.3%).

7. TEM image of CPT-loaded HSBNPs

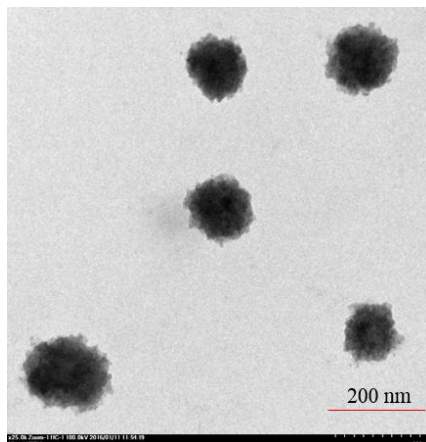


Figure S8. TEM image of CPT-loaded HSBNPs.

8. Photograph of the aqueous solutions of HA-SS-BFVPBT, free CPT and CPT-loaded HSBNPs

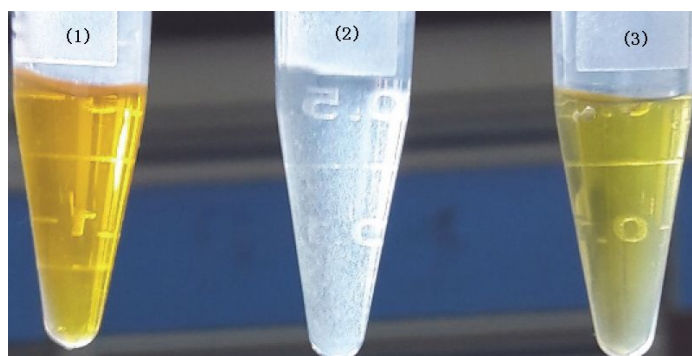


Figure S9. Aqueous solutions of (1) HA-SS-BFVPBT (2 mg/mL), (2) free CPT (0.1 mg/mL) and (3) CPT-loaded HSBNPs (1 mg/mL).

9. Stability of CPT-loaded HSBNPs under physiological conditions

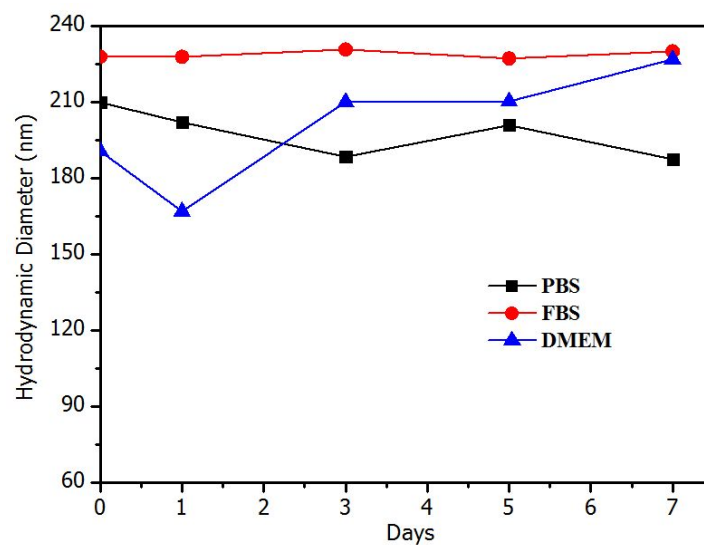


Figure S10. Particle size of CPT-loaded HSBNPs in PBS, FBS, and DMEM during 7 day storage at 25 °C.

#### 10. Photostability of HSBNPs in two-photon fluorescence cell imaging

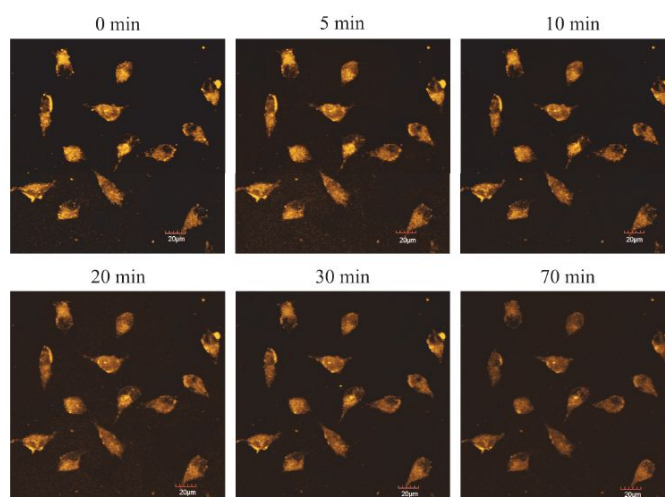


Figure S11. CLSM images of HeLa cells treated with HSBNPs after continuous irradiation for various durations with two-photon laser at 720 nm ( $0.6 \text{ w/cm}^2$ ).

#### 11. Control experiments for the detection of singlet oxygen

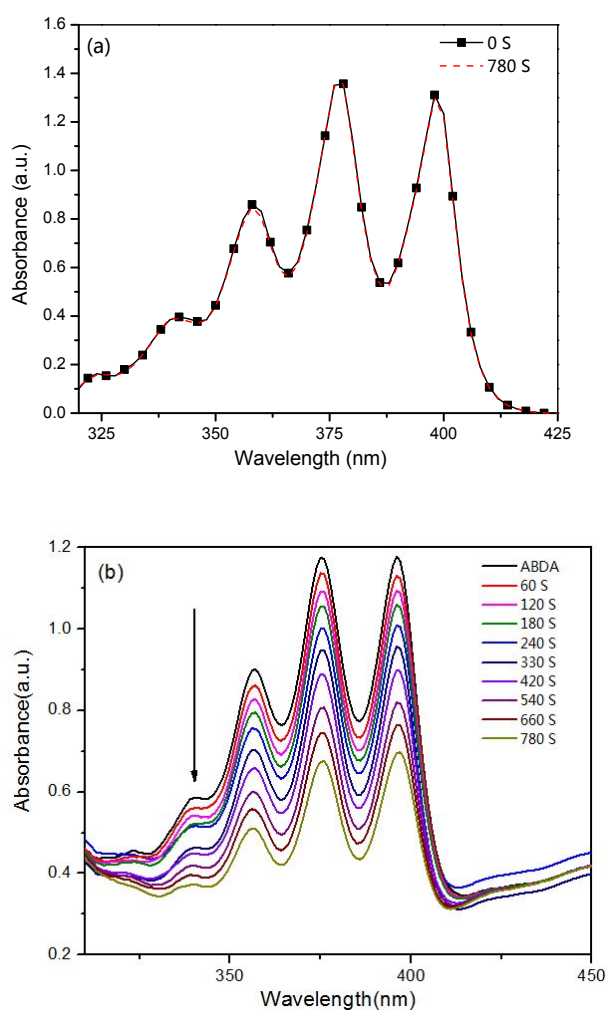


Figure S12. (a) UV-Vis absorption spectra of  $^1\text{O}_2$  trapping agent ABDA alone in aqueous solution before and after irradiation for 780 S. (b) UV-Vis absorption spectra of  $^1\text{O}_2$  trapping agent ABDA with  $\text{Ru(II)(bpy)}_3\text{Cl}_2$  in aqueous solution under irradiation for different irradiation time.

## 12. Cytotoxicity of HSBNPs against HeLa cells

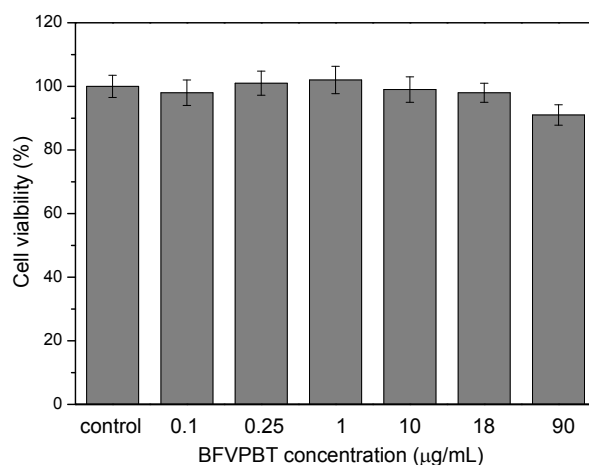


Figure S13. Cytotoxicity of HSBNPs against HeLa cells as a function of equivalent BFVPBT concentration by typical MTT assay.

## References

1. Pawlicki, M.; Collins, H. A.; Denning, R. G.; Anderson, H. L., Two-Photon Absorption and the Design of Two-Photon Dyes. *Angewandte Chemie-International Edition* **2009**, *48* (18), 3244-3266.
2. Yao, S.; Belfield, K. D., Two-Photon Fluorescent Probes for Bioimaging. *European Journal of Organic Chemistry* **2012**, (17), 3199-3217.
3. Pu, K.-Y.; Li, K.; Zhang, X.; Liu, B., Conjugated Oligoelectrolyte Harnessed Polyhedral Oligomeric Silsesquioxane as Light-Up Hybrid Nanodot for Two-Photon Fluorescence Imaging of Cellular Nucleus. *Advanced Materials* **2010**, *22* (37), 4186-4189.
4. Yue, X.; Morales, A. R.; Githaiga, G. W.; Woodward, A. W.; Tang, S.; Sawada, J.; Komatsu, M.; Liu, X.; Belfield, K. D., RGD-conjugated two-photon absorbing near-IR emitting fluorescent probes for tumor vasculature imaging. *Organic & Biomolecular Chemistry* **2015**, *13* (43), 10716-10725.
5. Wang, G.; Zhang, X.; Geng, J.; Li, K.; Ding, D.; Pu, K.-Y.; Cai, L.; Lai, Y.-H.; Liu, B., Glycosylated Star-Shaped Conjugated Oligomers for Targeted Two-Photon Fluorescence Imaging. *Chemistry-a European Journal* **2012**, *18* (31), 9705-9713.
6. Yu, D.; Zhang, Y.; Liu, B., Interpolyelectrolyte complexes of anionic water-soluble conjugated polymers and proteins as platforms for multicolor protein sensing and quantification. *Macromolecules* **2008**, *41* (11), 4003-4011.
7. Pu, K.-Y.; Li, K.; Liu, B., A Molecular Brush Approach to Enhance Quantum Yield and Suppress Nonspecific Interactions of Conjugated Polyelectrolyte for Targeted Far-Red/Near-Infrared Fluorescence Cell Imaging. *Advanced Functional Materials* **2010**, *20* (17), 2770-2777.
8. Cho, H.-J.; Yoon, H. Y.; Koo, H.; Ko, S.-H.; Shim, J.-S.; Lee, J.-H.; Kim, K.; Kwon, I. C.; Kim, D.-D., Self-assembled nanoparticles based on hyaluronic acid-ceramide (HA-CE) and Pluronic (R) for tumor-targeted delivery of docetaxel. *Biomaterials* **2011**, *32* (29), 7181-7190.
9. Huang, Y.; Yao, X.; Zhang, R.; Lang, O.; Jiang, R.; Liu, X.; Song, C.; Zhang, G.; Fan, Q.; Wang, L.; Huang, W., Cationic Conjugated Polymer/Fluoresceinamine-Hyaluronan Complex for Sensitive Fluorescence Detection of CD44 and Tumor-Targeted Cell Imaging. *Acs Applied Materials & Interfaces* **2014**, *6* (21), 19144-19153.